

YALE PEABODY MUSEUM

P.O. BOX 208118 | NEW HAVEN CT 06520-8118 USA | PEABODY.YALE. EDU

JOURNAL OF MARINE RESEARCH

The *Journal of Marine Research*, one of the oldest journals in American marine science, published important peer-reviewed original research on a broad array of topics in physical, biological, and chemical oceanography vital to the academic oceanographic community in the long and rich tradition of the Sears Foundation for Marine Research at Yale University.

An archive of all issues from 1937 to 2021 (Volume 1–79) are available through EliScholar, a digital platform for scholarly publishing provided by Yale University Library at <https://elischolar.library.yale.edu/>.

Requests for permission to clear rights for use of this content should be directed to the authors, their estates, or other representatives. The *Journal of Marine Research* has no contact information beyond the affiliations listed in the published articles. We ask that you provide attribution to the *Journal of Marine Research*.

Yale University provides access to these materials for educational and research purposes only. Copyright or other proprietary rights to content contained in this document may be held by individuals or entities other than, or in addition to, Yale University. You are solely responsible for determining the ownership of the copyright, and for obtaining permission for your intended use. Yale University makes no warranty that your distribution, reproduction, or other use of these materials will not infringe the rights of third parties.



This work is licensed under a Creative Commons Attribution-NonCommercial-ShareAlike 4.0 International License.
<https://creativecommons.org/licenses/by-nc-sa/4.0/>



Synoptic estimates of air-sea fluxes

by Richard F. Marsden^{1,2} and Stephen Pond¹

ABSTRACT

Synoptic and climatological dynamic studies generally rely on bulk aerodynamic flux formulae to describe air-sea heat and momentum exchange on synoptic and climatological scales. Barometric pressure maps (which involve an intrinsic spatial and temporal averaging of the wind) and wind roses provide two sources of spatial and temporal wind information for flux calculations. Several investigators have shown that time-averaged estimates of the fluxes based on vector-averaged winds systematically underestimate the actual time-averaged fluxes.

Using surface meteorological observations from 9 weatherstations in the North Atlantic Ocean and 2 weatherstations in the North Pacific Ocean, the three hourly stresses, latent heat fluxes and sensible heat fluxes were calculated. The sampled data and the calculated fluxes were then averaged over periods up to 28 days. The estimates of the averaged fluxes based on the vector-averaged winds were then compared to the directly averaged values. An upper bound for the difference in the two stresses calculations was directly proportional to the sum of the x and y component wind variances lost through the averaging process (in agreement with Fofonoff, 1960) and inversely proportional to the square of the vector-averaged wind speed. The wind-averaged and directly averaged flux estimates were grouped according to the Beaufort wind speed category and the averaging period. A multivariate regression was then performed to optimize a transformation from the wind-averaged to the directly averaged case. For all fluxes, the transformation dramatically improved the wind-averaged estimates of the climatological means and variances of the directly averaged fluxes. The residual error between the two estimates was decreased up to a factor of 5 over the uncorrected case and the correlation coefficients showed a moderate increase. The regression coefficients showed similar values for all temperate latitude stations.

An empirical formula was found which interpolated the wind speed and averaging period dependences and duplicated the multivariate regression results. The data from the ten temperate latitude stations were grouped and a single formula was found which only moderately increased the errors between the wind-averaged and directly averaged estimates. The geographically averaged formula was not applicable at Station N, located at the northern extremity of the North Pacific Trade Wind region.

Analysis of the 28 day wind-averaged flux spectral estimates showed that they underestimated the 28 day directly averaged flux spectral estimates. Application of the specific ship empirical formula greatly improved agreement between the two spectral densities and reduced the residual series power density at all frequencies. High latent heat flux errors at Station N were reduced by application of a seasonal correction.

1. Department of Oceanography, University of British Columbia, Vancouver, B.C., Canada, V6T 1W5.

2. Present address: Royal Roads Military College, Victoria, B.C., Canada, V0S 1B0.

1. Introduction

The most prevalent method of estimating transports of heat, moisture and momentum from the sea to the air on time scales longer than one hour has been through the bulk aerodynamic flux formulae (Roll, 1965). The fluxes, through dimensional considerations are proportional to the horizontal wind speed magnitude times the sea-air difference in heat, humidity or easterly or northerly wind.

Long time-scale flux estimates can be broken into two main groups. Climatological estimates of the long-term flux or of a long-term mean annual cycle are calculated from the average of many years of data. Two methods are used to calculate the climatological fluxes. First, from direct ship observations individual estimates of the fluxes are made and an average flux is directly calculated (Bunker, 1976). Second, wind roses are used to estimate the average wind speed magnitude and the flux is assumed to be equal to the average wind speed times the average temperature or humidity difference. In the case of stress, the calculations become more complex as the directional distribution must be taken into account (see Hellerman, 1965). The two methods are equivalent if the mean wind speed magnitude estimates calculated from the wind roses are accurate and if the covariances between the wind speed and the temperature, humidity and wind components (when separated into direction categories) are small compared to the product of the means. Marsden (1980) has shown that the two methods agree quite closely using data from 11 weatherships.

The second group are synoptic scale estimates. Here one attempts to follow the time history of the flux field development on temporal scales from about 0.25 to 28 days. Sea-surface barometric pressure maps are used to estimate geostrophic surface winds which are then converted to surface winds and used in flux calculations. The maps are inherently spatially and temporally averaged. Consequently the wind speed estimates have been component or vector-averaged. A vector-averaged estimate of the wind speed will be less than the average of the wind speed magnitudes over the same period since the wind speed is positive definite while the components may alternate positive and negative and cancel. Thus one expects that fluxes calculated from barometric pressure maps will underestimate directly averaged fluxes. Fofonoff (1960) used monthly averaged barometric pressure maps to calculate geostrophic currents in the North Pacific Ocean. He suggested that the difference between the directly averaged and vector-averaged flux estimates may be proportional to the sum of the variance of the x and y components of the pressure gradient over the monthly period. Malkus (1962) examined 59 three-hourly sampled wind observations from the Caribbean Sea and found that the vector-averaged stress underestimated the directly averaged stress by about 7%. Similar calculations at Ocean Weather-station C revealed that the vector-averaged stress was only 35% of the directly calculated value. She attributed differences in the reduction factor at the two locations to different variabilities in the winds between the Westerlies and the Trade Wind regimes. In the Trades, the winds are much steadier and long-period averages

are more indicative of short-term synoptic conditions. Over middle latitude oceans, the winds are much more variable, being dominated by storms with periods of a few days. Thus, long-period wind averages do not adequately indicate shorter period activity. Using six-hourly sampled barometric pressure maps in the Greenland Sea, Aagaard (1970) found that the Sverdrup transports based on directly averaged stresses for February 1965 were two to four times larger than those obtained from averaging the six-hourly pressures over the same period.

Esbensen and Reynolds (1981) found good agreement between the monthly averaged sensible and latent heat fluxes and an estimate of the heat fluxes based on the product of the monthly averaged wind speed and the monthly averaged air-sea temperature or air-sea humidity differences. This result is due to the covariances being small compared to the product of the means. Their approach is not applicable without corrections for the wind stress where covariances between the wind speed and the wind components are comparable to the product of the means. Fissel *et al.* (1977) show that these conditions are true at Station PAPA.

This study will attempt to quantify the errors that are inherent in flux calculations based on vector-averaged winds. From extensive three-hourly observations at eleven weatherstations in the North Atlantic and North Pacific Oceans, the stresses, and latent and sensible heat fluxes based on vector-averaged winds and the directly averaged air-sea fluxes will be calculated, compared, and transformations will be proposed to achieve more accurate flux estimates from vector-averaged winds.

2. Data

The data for the study consisted of three-hourly sampled observations of surface wind speed and directions, barometric pressure, air temperature, dew-point temperature and sea-surface temperature at nine locations in the North Atlantic Ocean (Ocean Weatherstations A, B, C, D, E, I, J and M) and at Ocean Weatherstations P and N in the North Pacific Ocean. The record length varied from a minimum of 10 years of data at Station P to a maximum of 22 years of data at Station N with a mean of approximately 16 years per ship. The station locations appear in Figure 1. Missing and obviously erroneous data were replaced by linear interpolation. For any variate with more than 125 consecutive incorrect values, the entire year of data for that variate was eliminated from calculations. Further details of the smoothing procedures can be found in Marsden (1980).

The three-hourly values for the surface wind stress and latent and sensible heat fluxes are given by the bulk aerodynamic flux formulae:

$$\left. \begin{array}{l} \tau_x \\ \tau_y \end{array} \right\} = \rho C_d (u^2 + v^2)^{\frac{1}{2}} \left\{ \begin{array}{l} u \\ v \end{array} \right. \quad (1)$$

$$H_s = \rho C_p C_t (u^2 + v^2)^{\frac{1}{2}} \Delta T \quad (2)$$

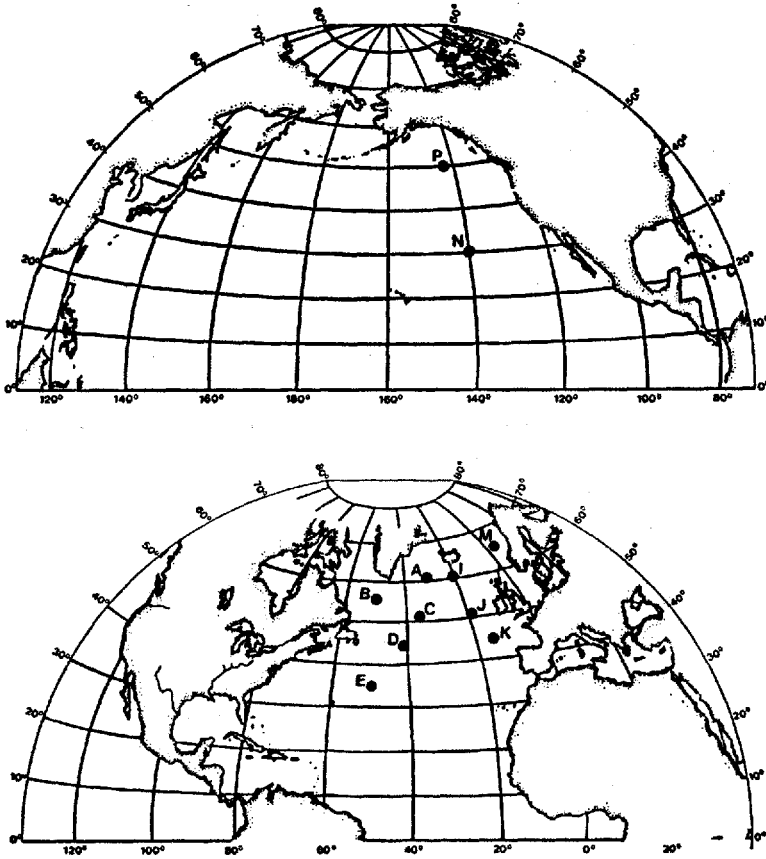


Figure 1. Ocean Weatherstation locations in the North Pacific and North Atlantic Oceans.

$$H_e = C_q E (u^2 + v^2)^{1/2} \Delta Q \quad (3)$$

where u and v are the three-hourly east and north wind components; ρ is the air density; ΔT is the sea-air temperature difference; ΔQ is the sea-air absolute humidity difference; C_p is the specific heat of air at constant pressure ($1.0 \times 10^3 \text{ J kg}^{-1} \text{ C}^{-1}$); E is the latent heat of evaporation of water ($2.46 \times 10^6 \text{ J kg}^{-1}$); C_d , C_t and C_q are the transfer coefficients known as the drag coefficient, the Stanton number, and the Dalton numbers respectively; τ_x and τ_y are the east and north stress components; H_s is the sensible heat flux; and H_e is the latent heat flux. A constant of 1.5×10^{-3} (after Pond *et al.*, 1974) was used for the transfer coefficients. A linear form of the drag coefficient:

$$C_d = 1.14 \times 10^{-3} \quad \text{for} \quad 0.0 < (u^2 + v^2)^{1/2} < 10 \text{ m/sec.}$$

$$C_d = (0.49 + 0.065 (u^2 + v^2)^{1/2}) \times 10^{-3} \quad \text{for} \quad (u^2 + v^2)^{1/2} \geq 10 \text{ m/sec.}$$

after Large (1979) or Large and Pond (1981) was also investigated. Details of the air-density and absolute humidity calculations can be found in Marsden (1980).

The data were assumed to be measured at the standard height of 10.0 m above the sea surface and under conditions of neutral stability. This study will be concerned with the ratio of the directly averaged to the vector-averaged fluxes. Nonstandard height corrections require a multiplicative factor applied equally to both averagings which cancels (Fissel *et al.*, 1977). Furthermore, slightly unstable conditions usually prevail over the oceans. Given a typical air-sea temperature difference of 3°C and a windspeed of 10 m/s, the stress would be underestimated by about 10% (Smith, 1981 and Bunker, 1976). A reasonable estimate of anemometer height is about 20.0 m which leads to a 10.0% overestimation of the stress. Consequently, on average, the nonstandard height and stability corrections tend to cancel. Esbensen and Reynolds (1981) show that neglecting stability corrections leads to errors of 5% or less for the stresses on average. More recent estimates of C_i and C_q corrected to neutral conditions (Large and Pond, 1982) are reasonably represented by constants although there may be a weak wind speed effect proportional to Cd^1 . As we are concerned with ratios the fact that they are appreciably less than 1.5×10^{-3} does not affect the results; however, our absolute values are too large for the heat fluxes and for the stress for the constant drag coefficient by 20-25%. If absolute values are being calculated, correction for the observation height and stability on a point-by-point basis should be made. A method for making these corrections using a bulk estimate of stability is given in Large and Pond (1982).

3. Analysis

Eqs. 1-3 were used to calculate three-hourly flux estimates at all stations. The three-hourly fluxes, wind components, air densities, absolute humidity differences and air-sea temperature differences were then averaged in consecutive blocks of 2, 4, 8, 16, 32, 56, 112 and 224 data points corresponding to periods of 0.25, 0.5, 1, 2, 4, 7, 14 and 28 days. The flux from the vector-averaged winds was then recalculated for each averaging block and compared to the corresponding directly averaged flux. Henceforth the directly calculated flux will be referred to as the $3H$ (or three-hourly based) flux and the flux calculated using the vector-averaged winds will be referred to as the VA flux. The length of time over which the three-hourly data set was averaged will be referred to as the averaging period, will be denoted by the capital letter L and will be expressed in days.

In calculating the VA latent heat fluxes, the air-sea humidity differences and not the dew-point and sea-surface temperatures (from which they were derived) were averaged. The dew-point and sea-surface temperatures are, however, the more commonly measured variables. It can be shown, however, that the averaged humidity differences and the humidity differences calculated from averaged temperatures

differ by 2% or less for averaging periods of $L = 28.0$ days.

The errors inherent in the *VA* estimates of fluxes were examined in terms of errors in climatological means, errors in long-term variances and errors in individual stress estimates. Four statistical parameters were used to assess these errors. Defining the *3H* flux as X_j and the *VA* flux as X'_j , where j represents one individual averaging, the effectiveness of estimating the long-term climatological mean flux is given by the difference mean (*DM*) defined as:

$$DM = \left| \frac{1}{N} \sum_{j=1}^N (X_j - X'_j) \right| \quad (4)$$

where N is the total number of averagings available in a given averaging period. A measure of accuracy of the long-term mean flux variance is given by the difference variance, defined as:

$$DV = \frac{\sigma_x^2 - (\sigma'_x)^2}{\sigma_x^2} \quad (5)$$

where: $\sigma_x^2 = \frac{1}{N} \sum_{j=1}^N X_j^2 - \left(\frac{1}{N} \sum_{j=1}^N X_j \right)^2$ and $(\sigma'_x)^2 = \frac{1}{N} \sum_{j=1}^N (X'_j)^2 - \left(\frac{1}{N} \sum_{j=1}^N X'_j \right)^2$ and $(\sigma'_x)^2$ (6)

$$(\sigma'_x)^2 = \frac{1}{N} \sum_{j=1}^N (X'_j)^2 - \left(\frac{1}{N} \sum_{j=1}^N X'_j \right)^2 \quad (7)$$

σ_x^2 is the variance of the directly averaged (*3H*) flux and $(\sigma'_x)^2$ the *VA* flux variance. The ability to predict the *3H* flux variance on a point-by-point basis is given by the residual variance (*RV*) defined as:

$$RV = \frac{1}{N} \frac{(\sum (X_j - X'_j)^2 - (DM)^2)}{\sigma_x^2} \quad (8)$$

$1 - RV$ is the estimate of the hindcast skill (Davis, 1977) of the transformation and is the fraction of the *3H* variance that can be reproduced by the *VA* variate. The correlation coefficient (*CR*) determines the statistical dependence of the *3H* variate on the *VA* variate and is given as:

$$CR = \frac{\frac{1}{N} \sum_{j=1}^N X_j X'_j - \left(\frac{1}{N} \sum_{j=1}^N X'_j \right) \left(\frac{1}{N} \sum_{j=1}^N X_j \right)}{\sigma_x \sigma'_x} \quad (9)$$

DV and *RV* are normalized for ease of ship-to-ship comparison. An appropriate normalizing factor for *DM* would be the mean climatological *3H* flux. At certain locations, the mean climatological flux was near zero leading to abnormally large relative errors.

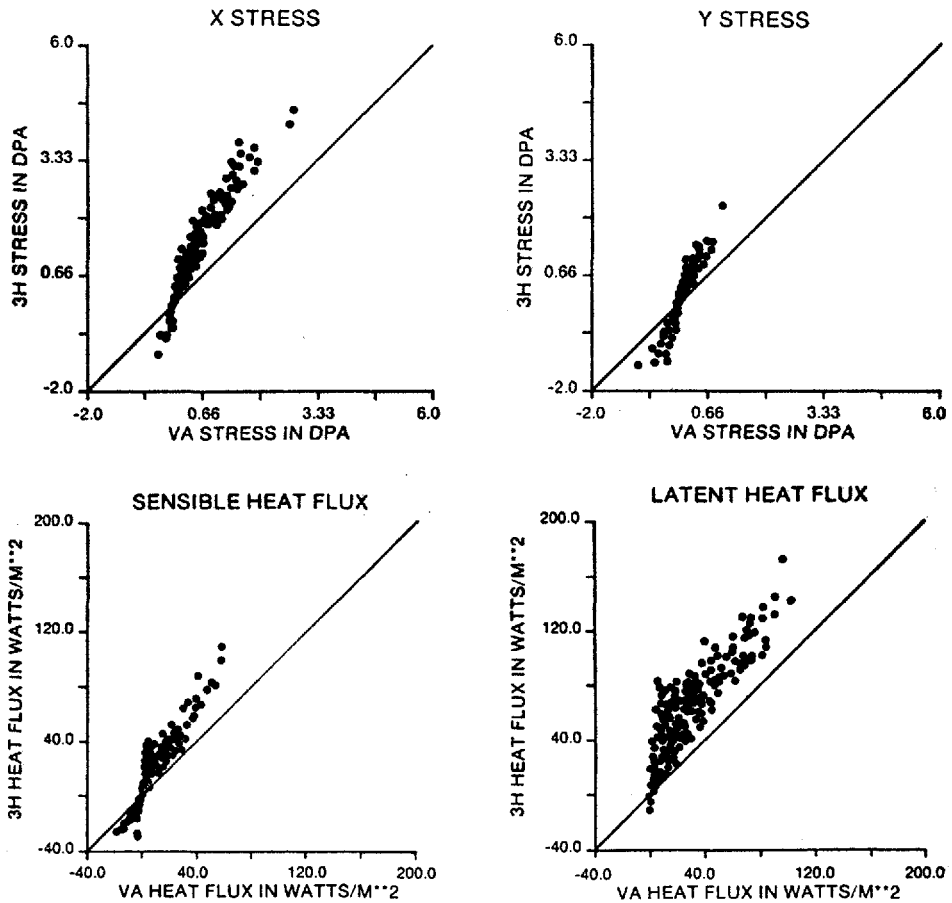


Figure 2. $3H$ versus VA stress (constant drag coefficient), and the sensible and latent $3H$ versus VA heat fluxes at Station C for $L = 28$ days.

The aims of this study were threefold: (a) to assess the inaccuracies inherent in the VA flux estimates; (b) to determine transformations which might improve VA flux estimates and; (c) to assess the improvements and accuracies of these transformations. To meet these aims, the four statistical parameters were calculated with no correction applied in order to define a raw error between $3H$ and VA fluxes. Next a multivariate statistical model was proposed to reduce the RV 's in an optimal manner. Finally, the model was applied to the data and the four statistical parameters were recalculated and were compared to the raw errors.

4. Raw errors

In Figure 2, the $3H$ fluxes found at Station C are plotted versus VA fluxes for

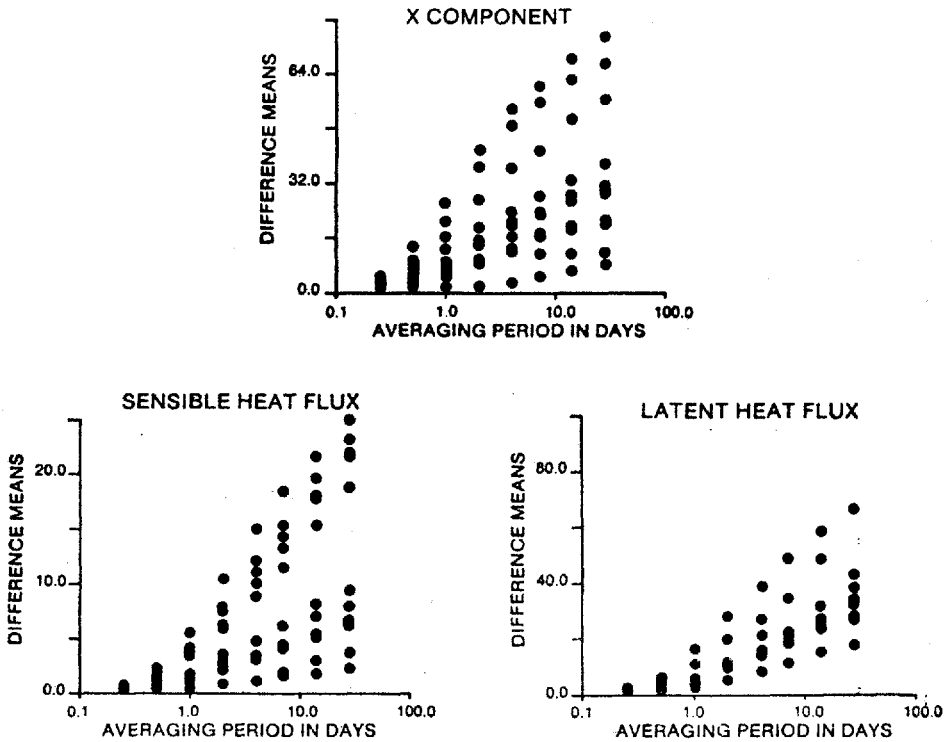


Figure 3. Example of the Difference Means for the fluxes with no corrections applied. The flux values are in milli Pascals (0.01 dynes/cm^2) for the stress (linear drag coefficient) and in Watts/m^2 for the heat fluxes. These errors are indicative of the climatological mean errors associated with raw VA flux estimates.

an averaging period of 28 days. The diagonal line indicates equivalence between the $3H$ and VA flux. In all cases the absolute value of the VA flux is consistently less than the $3H$ flux although the two variates are fairly well correlated. There is a bias toward positive heat fluxes, indicating a net transport from the ocean to the atmosphere. The heat fluxes appear to be less highly correlated than the stresses.

The raw difference means for the x component linear drag coefficient and for the heat fluxes are shown in Figure 3. DM 's are indicative of the inherent inaccuracies in using the VA flux for estimating the climatological mean fluxes. At all locations, the climatological errors increase with the averaging period. Furthermore, for each ship the DM error appears as a straight line with averaging period although the station location has not been explicitly indicated. The difference in the slopes of Figure 3 are dependent upon the mean $3H$ flux. The larger the mean $3H$ flux, the more rapidly the DM 's increase with averaging period. Station D has the largest mean errors (and hence the largest slope in the figure) for all three fluxes of 0.75 dPa

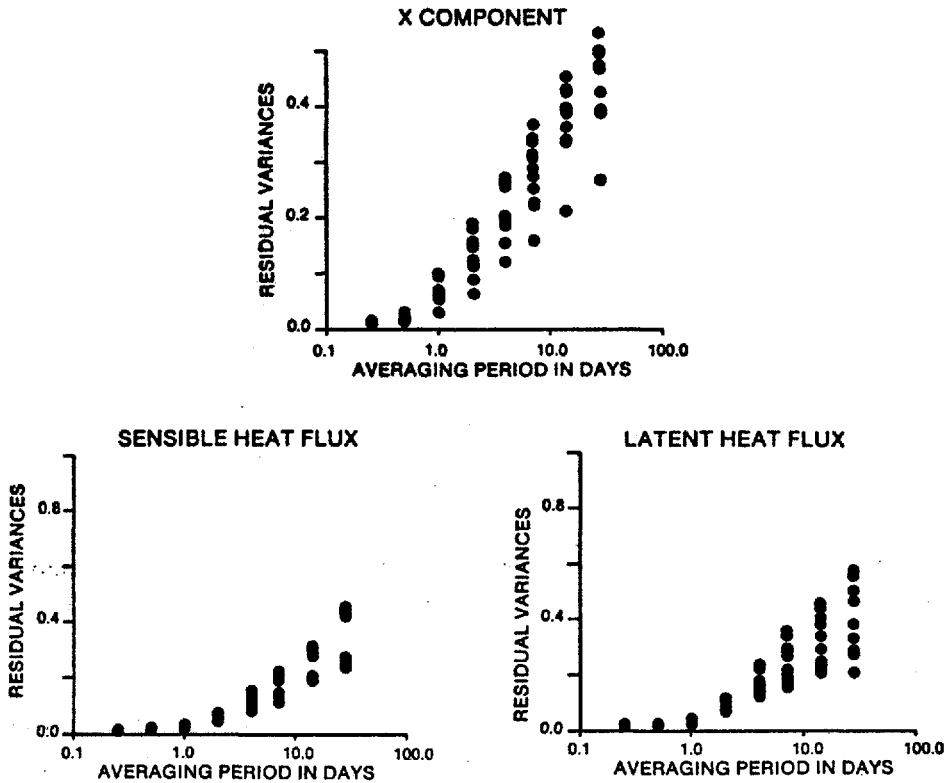


Figure 4. Example of the residual variances for the fluxes (linear drag coefficient for stress) with no corrections applied; the RV is normalized with the $3H$ variance. The RV for the latent heat flux at Station N for $L = 28$ days is 1.16 and is not shown.

(deci Pascals are used and are equivalent to dynes/cm²) for the x component of stress, 25 W/m² for the sensible heat flux and 74 W/m² for the latent heat flux for $L = 28$ days. These compare with mean $3H$ fluxes of 1.18 dPa for the stress, 46 W/m² for the sensible heat flux and 140 W/m² for the latent heat flux. Thus using monthly averages of the wind components can lead to mean errors as large as 55% of the mean flux value.

The uncorrected residual variances appear in Figure 4. For an averaging period of 0.25 days, the RV 's are less than 1% of the total $3H$ variance at all locations. The errors then increase with averaging period to about 40-50% error in the stresses, 25-45% error in the sensible heat fluxes and 20-60% error in the latent heat fluxes.

The difference variances and correlation coefficients will not be shown. Generally the DV 's increase from less than 1% at $L = 0.25$ days to maximum values at $L = 28$ days of 80-90% for the stresses, 60-70% for the sensible heat flux and 50-60 errors for the latent heat flux. The correlation coefficients are all greater than 0.9

Table 1. Beaufort wind speed intervals.

Beaufort #	Speed Interval	Mean Value m/sec
1	0.0- 0.4	0.2
2	0.4- 1.6	1.0
3	1.6- 3.4	2.5
4	3.4- 5.5	4.45
5	5.5- 8.0	6.75
6	8.0-10.8	9.4
7	10.8-13.9	12.35
8	13.9-17.2	15.55
9	17.2-20.8	19.0
10	20.8-24.5	22.65
11	24.5-28.5	26.5
12	28.5-33.5	31.0
13	> 33.5	35.0

for the stresses, 0.8 for the sensible heat fluxes and 0.6 for the latent heat fluxes. Further details of the inherent VA errors can be found in Marsden (1980).

5. Multivariate regression analysis

Assuming a constant drag coefficient, it can be shown (Marsden, 1980) that the ratio of the $3H$ stress magnitude to the VA stress magnitude for each averaging has an upper bound given by:

$$R_j(L) < 1 + (\sigma_{u_j^2} + \sigma_{v_j^2}) / (u_j^2 + v_j^2)^{1/2} \quad (10)$$

where $R_j(L)$ is the j th ratio of averaging period L , $\sigma_{u_j^2} + \sigma_{v_j^2}$ is the variance of the wind speed lost to the averaging, and $u_j^2 + v_j^2$ is the square of the vector-averaged wind speed over the averaging period. This suggests that the transformation from VA to $3H$ variates may depend upon vector-averaged wind speed.

For each VA flux calculated, the vector-averaged wind speed $(u_j^2 + v_j^2)^{1/2}$ was determined and the VA and $3H$ fluxes were further sorted into thirteen divisions according to the corresponding Beaufort category. The Beaufort wind speed categories according to the Marine Climatic Atlas, U.S. Office of Naval Operations, were used and are given in Table 1.

For every averaging period, an estimate of the $3H$ flux was obtained from the model:

$$\hat{X}_{jk}^l = \xi_k^l X'_{jk}^l \quad (11)$$

where \hat{X}_{jk}^l is j th flux estimate of Beaufort category k for averaging period l , ξ_k^l is the correction factor dependent on averaging period and wind speed and X'_{jk}^l is the j th estimate of the VA flux for Beaufort category k and averaging period l .

Using standard least squares techniques, the residual:

$$\sigma^2 = \sum_{k=1}^{13} \sum_{j=1}^{J_k} (X_{jk} - \xi_k X'_{jk})^2 \quad (12)$$

(where X_{jk} is the $3H$ flux, and J_k is the total number of averagings in Beaufort category k) was minimized giving:

$$\xi_k = \frac{\sum_{j=1}^{J_k} X_{jk} X'_{jk}}{\sum_{j=1}^{J_k} (X'_{jk})^2} \quad (13)$$

to give an optimal estimate of the transformation ξ_k .

It can be demonstrated (see Marsden, 1980) that, on average, there is no change in direction between the $3H$ and VA stress. Consequently the stress magnitudes were regressed giving a single correction applicable to both the x and y stress components. The sensible heat and latent fluxes were regressed separately.

It can be shown that for the optimal ξ_k transformation, the residual variances and difference variances are identical, leading to a positive bias in the DV 's. However, we wish to predict the long-term variance accurately. The problem was rectified by replacing ξ_k by:

$$\xi'_k = \xi_k x \left(\frac{1}{2} \right) \left(\frac{\sigma_x}{\sigma'_x} + \frac{\sigma_y}{\sigma'_y} \right) \quad (14)$$

for the stress and

$$\xi'_k = \xi_k \frac{\sigma}{\sigma'} \quad (15)$$

for the heat fluxes, where σ and σ' are the $3H$ and corrected VA variances respectively. This now forces the DV near 0.0% but increases the RV from its minimum value. Marsden (1980) gives an explicit formula for the increase which in all cases is less than +1%.

The optimal values of ξ_k were calculated and corrected for DV bias. Tables of the results including confidence intervals can be found in Marsden (1980). It was found that the ξ_k values for Station N for all fluxes were smaller than those found at the other 10 Stations. Furthermore the Station K sensible heat flux values were also smaller than the norm of the other ships. Station N is at the northern extremity of the summer trade wind regime in the North Pacific Ocean and the winds are characterized by a much lower variance in the summer (Dorman, 1974). Thus, the lower values are consistent with those found by Malkus (1962) in the Caribbean Sea and are consistent with the decreased upper bound of Eq. 10. The Station K results are, however, anomalous.

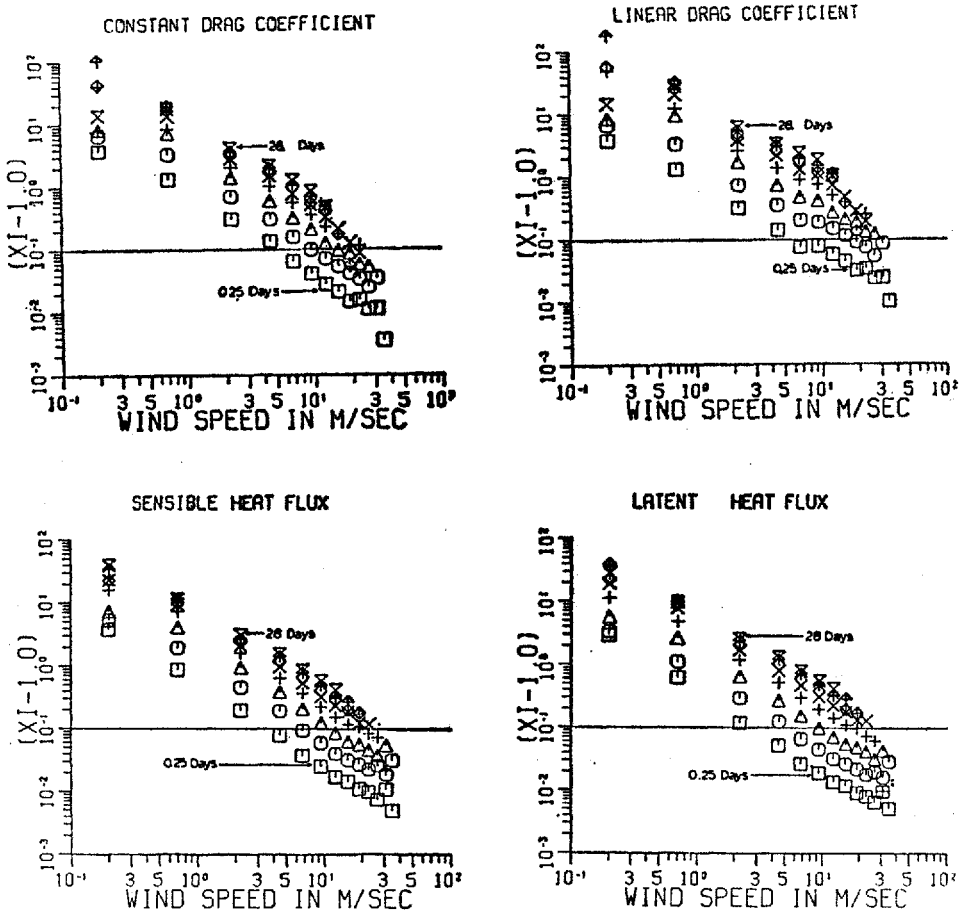


Figure 5. The $(\bar{\xi}_k^i - 1)$ values as a function of wind speed. For points above the horizontal line the raw VA fluxes require greater than 10% correction. The inset numbers indicate averaging period in days.

Between ships, the number of estimates within Beaufort category and averaging period varied due to inequalities in amounts of data per ship and due to differences in wind speed distributions. A geographically averaged $\bar{\xi}_k^i$ was calculated by applying weights proportional to the number of estimates with each Beaufort/averaging period category to each station and to the individual ships' ξ_k^i estimates. The difference $(\bar{\xi}_k^i - 1)$ was plotted versus vector-averaged wind speed $(u_j^2 + v_j^2)^{1/2}$ on logarithmic axes and the results appear in Figure 5. The curves are linear in the range 0.5 to 10.0 m/sec except for the linear drag coefficient case where some change in the slope may occur at 10 m/sec, the wind speed at which the drag coefficient changes form. Deviations from linearity occur for wind speeds greater than

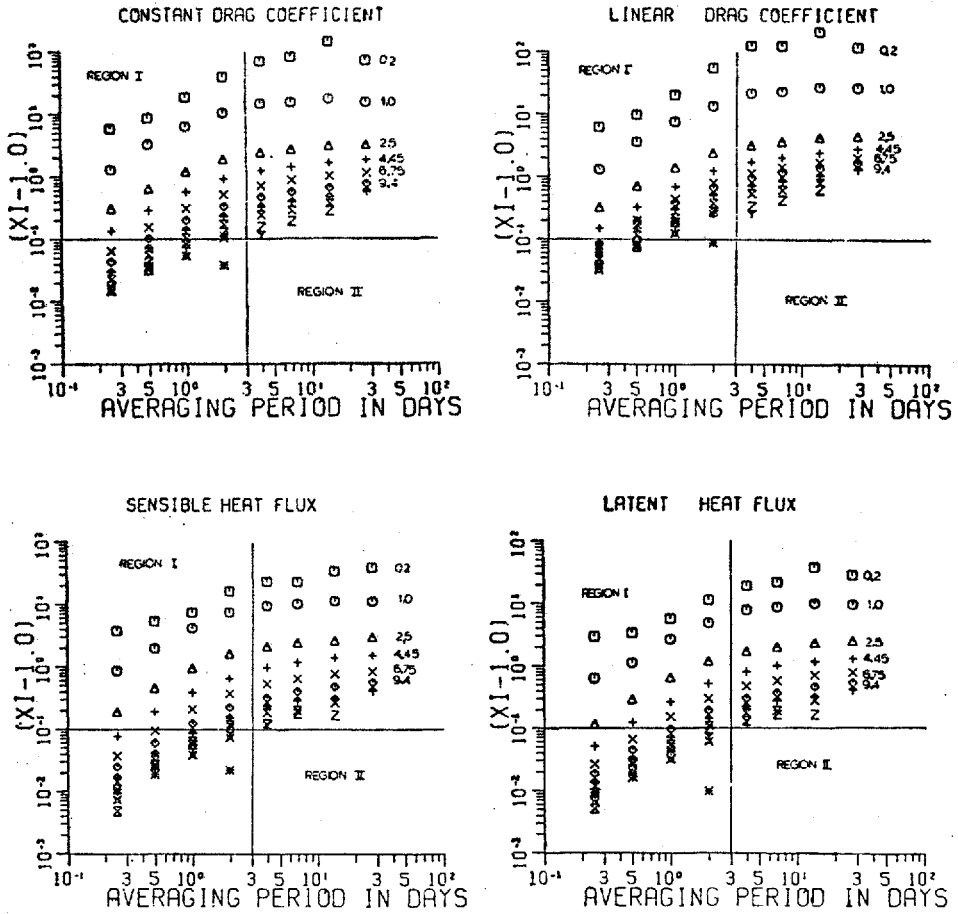


Figure 6. The $(\xi_k^i - 1)$ values as a function averaging period. The vertical line demarcates the division between Regions I and II. Above the horizontal line corrections larger than 10% are indicated. The inset numbers indicate wind speed in m/sec.

20 m/sec. This may be due to there being substantially fewer averagings at high wind speeds. The slopes for all curves appear to be similar for all averaging periods. The individual ships' plots of $(\xi_k^i - 1)$ versus $(u_j^2 + v_j^2)^{1/2}$ were examined and were all qualitatively similar to the geographically averaged case.

Next, $(\xi_k^i - 1)$ was plotted versus averaging period (L) on a logarithmic axis and the results appear in Figure 6. Again all fluxes show similar patterns. Beaufort interval 1 (0.2 m/sec) is more scattered than the others. This extends to Beaufort interval 2 (1.0 m/sec) on the individual ships $(\xi_k^i - 1)$ versus L plots. This is not surprising since the extremities in wind speed contain the fewest number of points

and the lowest wind speeds have the largest inherent errors. At $L = 2.0$ days, the * represents Beaufort category 12 (26.0 m/sec) and appears distinct from the pattern of the rest of the points. This point was determined from only four out of approximately one million total possible averagings and cannot be considered statistically valid. All other curves appear to increase systematically. From $L = 0.25$ to $L = 2.0$ days (which will be named Region 1) the slopes do not appear to change dramatically from one Beaufort category to the next.

Figure 5 indicates a power law behavior of $(\bar{\xi}_i - 1)$ with wind speed which appears to be independent of averaging period and Figure 6 indicates a power law behavior of $(\bar{\xi}_{ii} - 1)$ with averaging period which appears to be independent of wind speed. It is assumed *a priori* that an appropriate correction for the VA flux is through a factor

$$\eta = 1 + \alpha(u_j^2 + v_j^2)^{\beta/2} L^\gamma \quad (16)$$

where $(u_j^2 + v_j^2)^{1/2}$ is the vector averaged wind speed and L is the averaging period in days. The resultant $X(3H)$ and $X'(VA)$ residual is:

$$\delta^2 = \overline{(X - \eta X')^2} \quad (17)$$

where the overbar indicates averaging over all Beaufort categories and averaging periods. Eq. (17) can be rewritten as:

$$\delta^2 = \overline{[(X - X') - \alpha(u_j^2 + v_j^2)^{\beta/2} L^\gamma X']^2} \quad (18)$$

The parameters α , β and γ were chosen to minimize δ^2 by techniques outlined in Marsden (1980). α was then adjusted slightly to force the DV to zero as before.

Since Figure 6 indicated a definite break in the slope at $L = 3.0$ days, the regression was performed piecewise with a separate set of constants for the two regions. A regression of this type greatly reduces the required number of constants; consequently a separate regression was performed on the x and y stress components. Thus the number of parameters was reduced from 104 ξ_k^1 values per ship to 12 parameters for the stresses and 6 parameters for each of the heat fluxes. Even so, the residuals (δ^2) from the nonlinear regression yielded virtually identical or superior (i.e., smaller) residuals in every averaging period to those of the multivariate regression of Eq. 12. The parameters α , β and γ were calculated first for each ship individually. Then all the three-hourly measured data were grouped together (excluding Station N) and geographically averaged estimates of α , β and γ were determined. The geographically-averaged values of α , β and γ excluding Station N for all fluxes and Station K for the sensible heat flux are given in Table 2. Individual ship values are given in Marsden (1980).

The four test functions were then calculated using both the ships' individual η and the geographically averaged $\bar{\eta}$. The difference means and residuals variances only will

Table 2. The α , β and γ values for the geographically averaged empirical formula equation $\bar{\eta} = 1 + (u_s^2 + v_s^2)^{\beta/2} L^\gamma$. With Station N excluded for all stresses and Station K excluded in the sensible heat flux, the Type column coding is as follows: τ_x —east component of stress, τ_y —north component of stress, H_s —sensible heat flux, H_L —latent heat flux, con—constant drag coefficient, lin—linear drag coefficient.

Type	Region I 25-20 days			Region II 4.0-28.0 days		
	α	β	γ	α	β	γ
τ_x con	3.337	-1.322	0.920	4.237	-1.150	0.261
τ_y con	3.437	-1.336	0.901	4.639	-1.183	0.231
τ_x lin	2.325	-0.910	0.967	3.276	-0.795	0.310
τ_y lin	2.322	-0.910	0.940	3.754	-0.853	0.275
H_s	2.874	-1.469	0.984	3.946	-1.244	0.244
H_L	1.365	-1.251	1.021	2.335	-1.108	0.263

be described. The difference means for the individual ships' η appear in Figure 7. Except for Station A, and at 28 days for Station B, all DM 's are below 0.08 dPa for the linear drag coefficient. The constant drag coefficient values are lower. The sensible heat flux DM 's, with the exception of Station I, $L = 28$ days are all less than 2.5 watts/m² while the latent heat fluxes are mostly less than 10 watts/m². These compare with climatological errors as large as 0.75 dPa for the stress components, 25 watts/m² for the sensible heat flux and 74 watts/m² for the latent heat flux with no correction. The residual variances appear in Figure 8. Generally, the linear drag coefficient RV 's increase with averaging period in Region I but are scattered about a constant in Region II. The x component RV 's are between 6-12% in Region II while the y component values (not shown) lie between 8-17%. The corresponding constant drag coefficient values are about one-half of the linear drag coefficient values. The sensible heat fluxes generally follow the pattern of the stress and, with the exception of Station N, are less than 8%. The latent heat fluxes are somewhat less accurate with all stations except E, M and N being less than 18%. Again a marked reduction from the uncorrected values has occurred.

The empirical formula permitted interpolation of the VA wind speed correction within each Beaufort category. When the empirical formula was applied to each VA estimate individually, certain ships showed a dramatic decrease in residual variance. For example, Station N latent heat flux had a ξ_k^1 RV of 82% for $L = 28$ days. When the empirical formula interpolated the velocities, the RV was only 59%. In the sensible heat flux, the change was from 23% to 13%. At $L = 28$ days, 78% of the data is grouped in Beaufort categories 3 and 4. Consequently the interpolation of the correction within the two groups was important. At locations where the data were more evenly distributed among Beaufort categories (e.g., Station C), the improvement by application of η to the VA flux was less than 1.0%.

Except at Station N the difference means using the geographically averaged $\bar{\eta}$ are

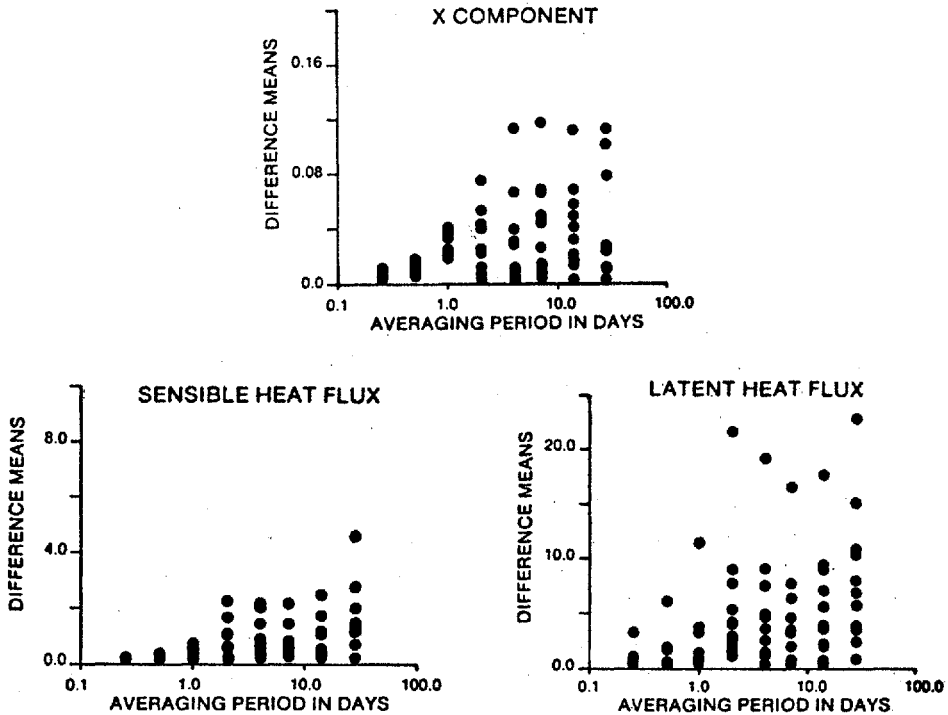


Figure 7. The difference means using the individual ships' empirical formula (η). The heat flux DM 's are in Watts/m² while the stress DM 's are in dPa (linear drag coefficient).

similar to those of the η results with most values being less than 0.08 dPa for the stress, and 2.5 and 10 watts/m² for the sensible and latent heat fluxes; the extreme values are 0.13 dPa, 2.9 and 14 watts/m², respectively. The inapplicability of $\bar{\eta}$ at Station N is readily evident in abnormally large DM values for all three fluxes (Marsden, 1980). The residual variances using the geographically averaged $\bar{\eta}$ are, with the exception of Station N, remarkably similar to the individual ship empirical formula $\bar{\eta}$ RV values. For the stresses and the sensible heat flux, the RV 's at all averaging periods are within 1% of the individual η values, except that the heat flux value at Station K shows a 5.0% increase at $L = 28$ days over the individually calculated value. This is consistent with the anomalous ξ_k^1 corrections in the sensible heat flux at Station K noted previously. For Station I at $L = 28$ days the latent heat flux RV is increased by 10% using $\bar{\eta}$; in all other cases the $\bar{\eta}$ RV 's are within 5% of the η values. The geographically averaged empirical formula approach, with two exceptions, appears to yield nearly identical results to the individual ships' empirical formula. This approach is not viable for any of the fluxes at Station N and may not be the best estimate for the Station K sensible heat flux correction.

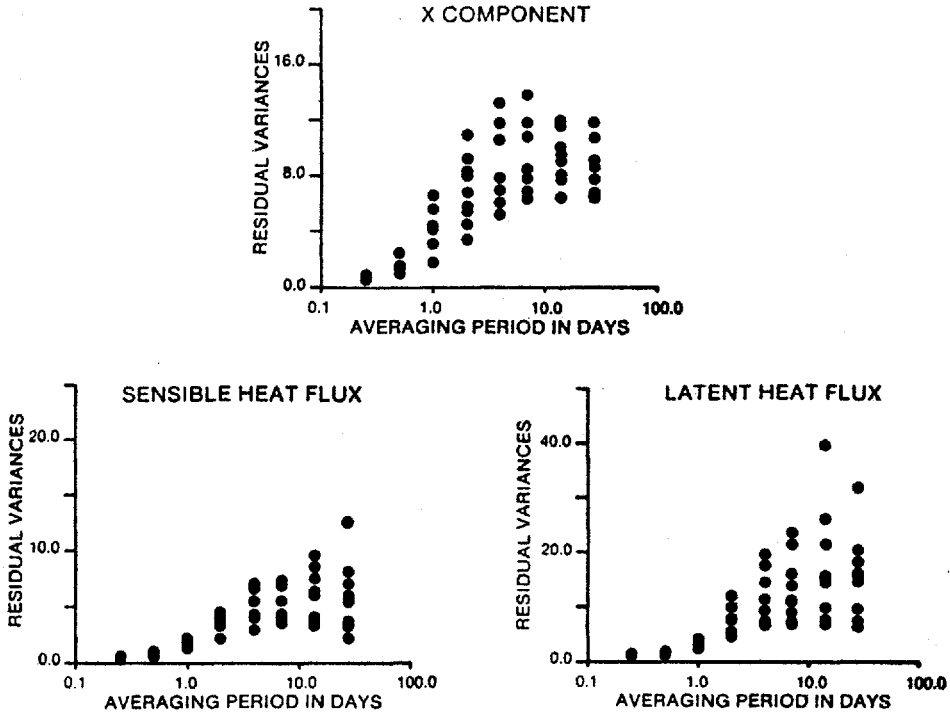


Figure 8. The residual variances with the individual ships' empirical formula (η) applied. Values are in percent. Linear drag coefficient for X stress component.

6. Seasonal corrections

The latent heat flux corrections at Station N are characterized by markedly larger residuals and lower correlation coefficients for averaging periods in Region II. When the empirical formula, η , is applied, at $L = 28$ days, the RV is 59% of the $3H$ variance. Although the sensible heat flux residuals are larger at Station N they are less pronounced than for the latent heat flux.

The required transformations may be inherently nonstationary. It has been assumed that the winter corrections, for example, are identical to the summer corrections. Dorman (1974) has demonstrated that at Station N there are large amounts of energy at the annual cycles for the winds, wind components, sea-surface temperatures, air temperatures and dew-point temperatures. Except for sea-surface temperatures, the character of all component variates changes markedly from winter to summer. For example, the winter clockwise wind component has more than four times the power of that of the summer component. Some of the scatter that is evident between the $3H$ and VA variates may be due to seasonal changes in the required corrections.

One method to determine whether the annual cycle plays a dominant role in the required corrections is to examine the $3H$ and VA and residual ($3H-VA$) spectra. To this end Station C was selected as a control because it exhibits particularly stable heat flux RV 's at $L = 28$ days—8% for the latent heat flux and 4% for the sensible flux as compared to 59% and 13% respectively at Station N after the ships' empirical formula, η , was applied. The data at both ships were averaged, and the lunar monthly $3H$, VA and residual stresses were calculated. The three time series were then broken into 9 two-year blocks at Station C and 10 two-year blocks at Station N. Each two-year block was detrended and a cosine taper was applied according to Bendat and Piersol (1971). The twenty-six points within each block were then fast fourier transformed by UBC FOURS program and the square of the magnitude of each fourier sine/cosine pair was calculated. The spectral density estimates for all blocks were added and the mean power density estimate was found.

The spectra for the heat fluxes at Stations C and N are shown in Figure 9. At Station C, for the sensible heat flux, the VA spectrum closely matches the $3H$ spectrum at all frequencies. At 0.5 cycles/year the VA spectrum slightly under-predicts the $3H$ spectrum while at 3.5 cycles/year, it slightly over-predicts the $3H$ spectrum. The over and under-predictions counter-balance accounting for a low 0.5% difference variance (DV). The residual spectral power is quite negligible at all frequencies compared to the $3H$ spectrum. The latent heat flux VA spectrum also closely approximates the $3H$ spectrum for all but the annual cycle. The 350 (watt/m²)² years difference at this frequency accounts for a large portion of the 3% DV . The residual spectrum shows a slight increase at the annual cycle but it cannot be classified as significant. Thus, even though there is substantial power in the $3H$ and VA variates at the annual cycle there is no indication of a substantial peak in the residual spectrum. At Station N, the sensible heat flux results approximate the $3H$ results reasonably well at all frequencies except the annual cycle where the VA results underestimate the $3H$ results. At 8 other harmonics, the VA series slightly overestimates the $3H$ series. In attempting to reduce the DV error to 0, the variance difference at the annual cycle may have been increased to the detriment of the other frequencies. The residual series shows a slight rise at the annual cycle but is probably not significant in comparison to the error at the other frequencies. In the latent heat flux at Station N, the VA series underestimates the $3H$ spectral densities at most frequencies. At the annual cycle, the residual power density is more than 4 times that at any other frequency. Thus seasonal corrections may be required at Station N in the latent heat flux and this residual power density is approximately equal to the sum of the VA and $3H$ powers.

The time series of the residual latent heat flux at Station N with η applied is shown in Figure 10. The annual cycle is evident. In contrast, the Station C residuals in Figure 10, as suggested in the spectra, show no dominant periodicity. An inspection of the data at Station N, $L = 28$ days, latent heat flux revealed that grouping

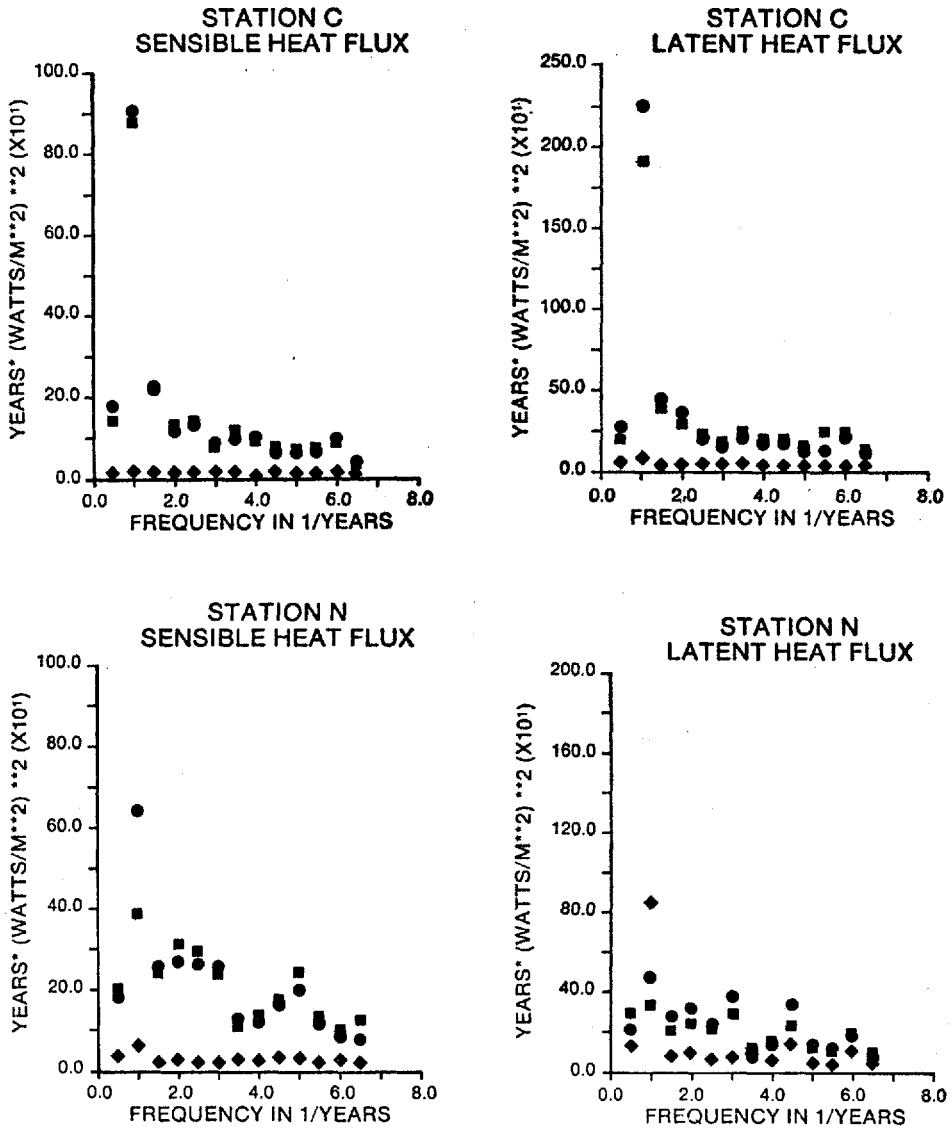


Figure 9. The spectra of the VA, residual and 3H heat fluxes at Stations C and N with η applied. The VA series is indicated by ■, the 3H series by ● and the residual series by ◆. The 95% confidence ranges are (0.57, 2.19) (Station C) and (0.59, 2.08) (Station N) times the value shown (18 and 20 degrees of freedom).

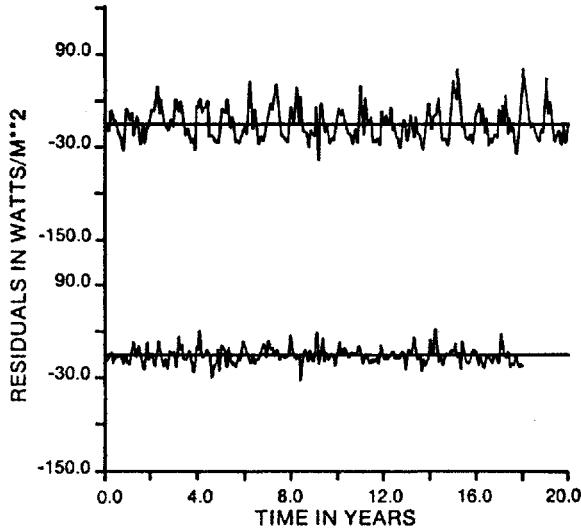


Figure 10. The corrected residual series at Stations N and C for the latent heat flux, $L = 28$ days.

months 1-5 and 11-13 inclusive reflected a positive bias in the residuals while months 6-10 inclusive reflected a negative bias in the residuals. The data were then arranged in these groups and a winter and summer empirical formula calculated for $L = 28$ days. The latent heat RV 's were calculated using these values and were reduced to 32%. Sensible heat RV 's were reduced to 8%.

Station D has the largest residuals for the y component, linear drag coefficient and the second largest residuals for the x component linear drag coefficient. Consequently, the spectra at this station were examined at $L = 28$ days. Figure 11 upper half shows the x and y component spectra calculated from the uncorrected time series. The x component $3H$ and residual spectra both show distinct increases in spectral density at the annual cycle while the y component is quite white. In both components the residual spectra are larger at all frequencies than the VA spectra indicating that the error is greater than the actual VA estimate of the power. This indicates that severe errors may arise if geostrophic winds from barometric pressure maps averaged over periods of greater than perhaps four days are used to calculate stress spectra. One expects much smaller errors in the spectra calculated by Willebrand (1978) since the errors for the 28-day averaging period shown here are much larger than those for the 12 hourly averaging period upon which he based his study.

Figure 11 lower half shows the VA and $3H$ spectra with η applied to the VA series. In the x component there is a definite mis-match between the $3H$ and VA spectra at the annual cycle while the residual spectrum shows a slight peak. At all other frequencies, however, the $3H$ and VA spectra match quite well. After correc-

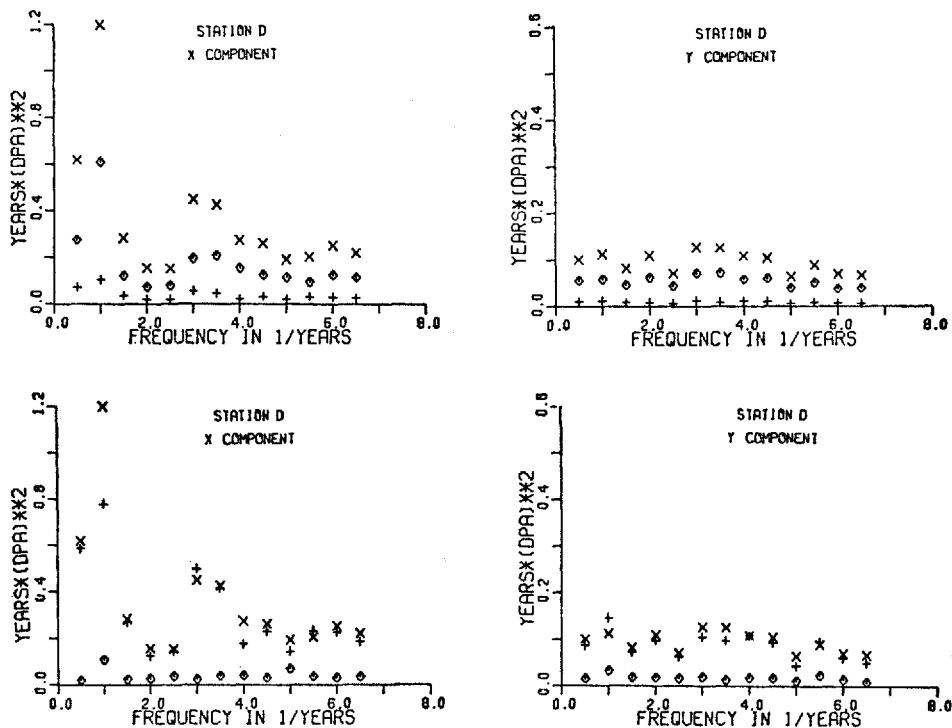


Figure 11. The x and y component power spectra, linear drag coefficient for the uncorrected (a) and corrected (b) VA series at Station D, $L = 28$ days. The confidence interval is (0.57, 2.19) times the value shown (18 degrees of freedom). VA series indicated by +, $3H$ by \times and the residual by \diamond .

tion, the y component $3H$ and VA match fairly well at all frequencies while the residual series is much lower in power.

The Station N residual series of latent flux shows a large amount of power at the annual cycle which can be reduced by applying a semiannual correction. This suggests that a time-dependent correction may be required for the stresses at Station N. The individual Station N stress correction for the linear drag coefficient was applied and the results are shown in Figure 12. Note that the scale on the y axis (spectral power density) has been increased by an order of magnitude over that for Station D (of Fig. 11). There is a slight mis-match of power between the $3H$ and VA series as well as a slight rise in the y component stress residual power density at the annual cycle.

The Station D x stress component and N y stress component are similar to the N sensible heat flux results. Use of seasonal correction would thus reduce the residual variance by about 50% (i.e., from 12% or less to 8% or less). Since the RV 's are fairly small, use of a seasonal correction does not seem worthwhile.

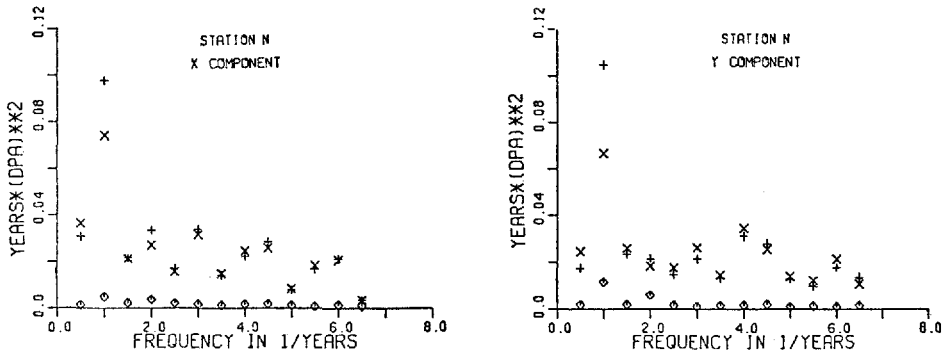


Figure 12. The stress spectra at Station N corrected with η . $L = 28$ days, linear drag coefficient. The 95% confidence limits are (0.59, 2.08) times the value shown (20 degrees of freedom). Symbols have same meaning as on Figure 11.

7. Conclusions

A systematic underprediction of the $3H$ air-sea fluxes (calculated from data at 3-hour intervals) occurs when they are estimated through VA (vector-averaged) parameters. The required transformations to correct for these losses are similar for all fluxes and are dependent upon the VA wind speed and upon averaging period. Four test functions: the difference means, difference variances, residual variances, and correlation coefficients were defined to quantify the differences between the VA and $3H$ fluxes. In all cases the difference means, difference variances, and residual variances increased with averaging period while the correlation coefficients showed a similar decrease. The residual variance (RV) measured the point-by-point differences and had maximum uncorrected values at $L = 28$ days of 30-40% for the stress (constant drag coefficient), 25-45% for the sensible heat flux and 30-60% (except for Station N 116%) for the latent heat flux.

One method of correcting for the $3H$ - VA discrepancies was to linearly regress the two variants as a Beaufort category/averaging period basis arriving at a transformation ξ_k^1 . Marked improvements were found in all four test quantities. The RV 's increased to 3 days and then remained fairly constant from 3 to 28 days. At $L = 28$ days, the constant drag coefficient RV 's were reduced to 5-8%, the linear drag coefficient RV 's were reduced to 5-15% (except for Station N 23%) and the latent heat flux RV 's were reduced to 10.0-50% (except for Station N 83%). Significant (>10.0%) corrections were required for all wind speed categories for averaging periods great than 0.5 days.

Plots of ξ_k^1 (geographically averaged values) indicated that the transformations may be quite regular over varying averaging periods and varying wind speeds for all fluxes. A nonlinear regression of the form $\eta = 1 + \alpha(u^2 + v^2)^{\beta/2}L^\gamma$ was performed and an analysis of the test quantities revealed that application of this formula

to the VA fluxes produced nearly identical results to the ξ_{kl} test results. The best method of application of the formula was to allow it to correct each VA estimate on a point-by-point basis. All ships excluding Station N for all fluxes and Station K for the sensible heat flux required similar corrections. The calculated difference means, residual variances, and correlation coefficients were insensitive to a geographic grouping of transformations.

The similarity of the results for all fluxes indicated that the vector averaging of the wind in general, and the loss of wind variance information in particular, determined the extent of the reduction for all fluxes. This was confirmed at Station N where a 10 fold reduction in wind speed variance accounted for markedly reduced corrections required for all three fluxes. The discrepancy at Station K, sensible heat flux, remains an enigma.

An analysis of the heat flux spectra at Stations C and N demonstrated some of the internal properties of the transformations. A large annual cycle in both the latent and sensible $3H$ heat fluxes did not necessitate a seasonal transformation at Station C where the residual variances were lowest. An analysis of the residual spectra at Station N, exactly where the heat flux residuals were highest, revealed that a seasonal transformation could markedly improve the residual variance. Thus, the gross form of the transformation may be dictated by the vector averaging of the wind; deviations from the broad transformations may be dependent upon correlation of the annual air-sea temperature or humidity differences with the annual winds.

An analysis of the uncorrected stress component spectra showed a consistent underestimation of the $3H$ spectra by the VA spectra at all frequencies. Even though Station D showed the highest residuals after transformations, the transformed VA spectra showed that a seasonal transformation would probably not improve the situation enough to be worthwhile.

Any one of the transformations (ξ_{kl}^l , η , $\bar{\eta}$) greatly improves calculations based on air-sea fluxes calculated from averaged constituent data. Application of the transformation should yield more accurate results from numerical models of the ocean circulation while using more realistic air-sea transfer coefficients. Furthermore, the technique offers the possibility of depicting the time history development of specific wind forced oceanic events. Given the similarity in the test function results between ξ_{kl}^l , η , $\bar{\eta}$ it would appear that the same correction ($\bar{\eta}$) can be applied *over the whole ocean in temperate latitudes*.

Several facets, particularly in applying transformations to barometric pressure, require further investigation. First, the barometric pressure maps have an inherent spatial averaging which could not be simulated in this study. Similar calculations at the eleven weathership locations based on geostrophic wind data (such as developed by Willebrand, 1978) could confirm whether similar transformations for geostrophic wind are applicable. Second, the subtropics, tropics, and monsoon regions (where a strong annual signal is inherent in the winds) have not been investigated.

Esbensen and Reynolds (1981) have shown that the *heat fluxes* using monthly mean values of wind *speed* and air-sea temperature and humidity differences can be calculated using uncorrected bulk coefficients. Variations of periods of a few months or more can be followed. The wind stress *cannot* be calculated using their method. Perhaps correction factors applicable to various geographic regions could be found but this question has not been investigated as far as we know.

For climatological flux values (including the seasonal cycle) wind roses and the standard bulk coefficients may be used with an uncertainty of 5% or less (Marsden, 1980) which is less than the uncertainty in the coefficients themselves.

Our method is for use with *vector-averaged* winds which would be obtained with suitable rotation and reduction from barometric pressure maps or from vector-averaged winds derived from cloud motions. The fluxes and their fluctuations of periods of a day or so and longer can be followed depending on the basic averaging period for the winds, usually with an uncertainty in the flux magnitude of 5-10% of the root mean square value. The uncertainty in mean values is usually 5-10% of the maximum magnitudes found in temperate regions.

Acknowledgments. The North Atlantic weathership data were supplied by Dr. R. Pollard of the Institute of Oceanographic Sciences, Wormley and the Station N data were obtained from Dr. C. Dorman, San Diego State University. Mr. B. Walker performed the initial structuring of the computer tapes. Dr. W. Large offered many practical suggestions in processing the large amounts of data involved. Dr. B. Ruddick aided greatly in producing the final figures.

The project was supported by the United States Office of Naval Research (Contract N00014-76-C-0446 under Project 083-207) and by the Natural Science and Engineering Research Council of Canada (Grant A8301).

RFM received personal support from an NSERC scholarship.

REFERENCES

- Aagaard, K. 1970. Wind-driven transports in the Greenland and Norwegian Seas. *Deep Sea Res.*, 17, 281-291.
- Bendat, J. S. and A. G. Piersol. 1971. *Random Data*. Wiley-Interscience, New York, 407 pp.
- Bunker, A. F. 1976. Computations of surface energy flux and annual air-sea interaction cycles of the North Atlantic Ocean. *Mon. Wea. Rev.*, 104, 1122-1140.
- Davis, R. E. 1977. Techniques for statistical analysis and prediction of geophysical fluid systems. *Geophys. Astrophys. Fluid Dyn.*, 8, 245-277.
- Dorman, C. E. 1974. Analysis of meteorological and oceanographic data from Ocean Station Vessel N (30N, 140W). Ph.D. thesis, Oregon State University, 136 pp.
- Esbensen, Steven K. and R. W. Reynolds. 1981. Estimating monthly-averaged air-sea transfers of heat and momentum using the bulk aerodynamic method. *J. Phys. Oceanogr.*, 11, 457-465.
- Fissel, D. B., S. Pond and M. Miyake. 1977. Computation of surface fluxes from climatological and synoptic data. *Mon. Wea. Rev.*, 105, 26-36.
- Fofonoff, N. P. 1960. Transport computation for the North Pacific Ocean. Ms. Rep. Ser., Fish. Res. Bd. Can., 77, 87 pp.
- Hellerman, S. 1965. Computations of wind stress over the Atlantic Ocean. *Mon. Wea. Rev.*, 93, 239-244.

- Large, W. G. 1979. The turbulent fluxes of momentum and sensible heat over the open sea during moderate to strong winds. Ph.D. thesis, Department of Oceanography, University of British Columbia, 180 pp.
- Large, W. G. and S. Pond. 1981. Open ocean momentum flux measurements in moderate to strong winds. *J. Phys. Oceanogr.*, *11*, 324–326.
- 1982. Sensible and Latent heat fluxes over the ocean. *J. Phys. Oceanogr.*, *12*, 464–482.
- Marsden, R. F. 1980. Synoptic estimates of air-sea fluxes. Ph.D. thesis, Department of Oceanography, University of British Columbia, 239 pp.
- Malkus, J. S. 1962. Large-scale interactions, *in* *The Sea* Vol. I, M. Hill, ed., Interscience Publishers, New York, 88–294.
- Pond, S., D. B. Fissel and C. A. Paulson. 1974. A note on bulk aerodynamic coefficients for sensible heat and moisture fluxes. *Boundary-Layer Meteorol.* *6*, 333–339.
- Roll, H. V. 1965. *Physics of the Marine Atmosphere*. Academic Press Inc., New York, 426 pp.
- Smith, S. D. 1981. Factors for adjustment of wind speed over water to a 10 metre height. Bedford Institute of Oceanography Report Series, BI-R-81-3, 29 pp.
- Willebrand, J. 1978. Temporal and spatial scales of the wind field over the North Pacific and North Atlantic. *J. Phys. Oceanogr.*, *8*, 1080–1094.